Structural Engineering of MXenes Frameworks with Abundant Surface Functionalities for Enhanced Lithium-Sulfur Battery Electrochemistry

Yongjie Ye[a], Sisi Liu[a], Yongqian He[a], Wanqi Zhang[a], Ying Chen[a], Mengqing Wang[a], Xuewen Peng [a], Caixiang Wang[a], Qin Tang[a], Yan Luo[a], Bing Wu[b,*], Hongbo Shu[a], Ruizhi Yu [c,*], Manfang Chen[a,*]

(a National Base for International Science & Technology Cooperation, National Local Joint Engineering Laboratory for Key Materials of New Energy Storage Battery, Hunan Province Key Laboratory of Electrochemical Energy Storage & Conversion, School of Chemistry, Xiangtan University, Xiangtan 411105, China;

b Department of Inorganic Chemistry, University of Chemistry and Technology Prague, Technická 5, Prague 6, 166 28 Czech Republic;

c Institute of Micro/Nano Materials and Devices, Ningbo University of Technology, Ningbo, Zhejiang 315211, China)

[*]E-mail: (Bing Wu) wui@vscht.cz (B. Wu), (Ruizhi Yu) ruizhi.yu@nbut.edu.cn, (Manfang Chen) mfchen@xtu.edu.cn;

[*] Corresponding authors.
E-mail addresses: wui@vscht.cz (B. Wu), ruizhi.yu@nbut.edu.cn (R. Yu), and mfchen@xtu.edu.cn (M. Chen)

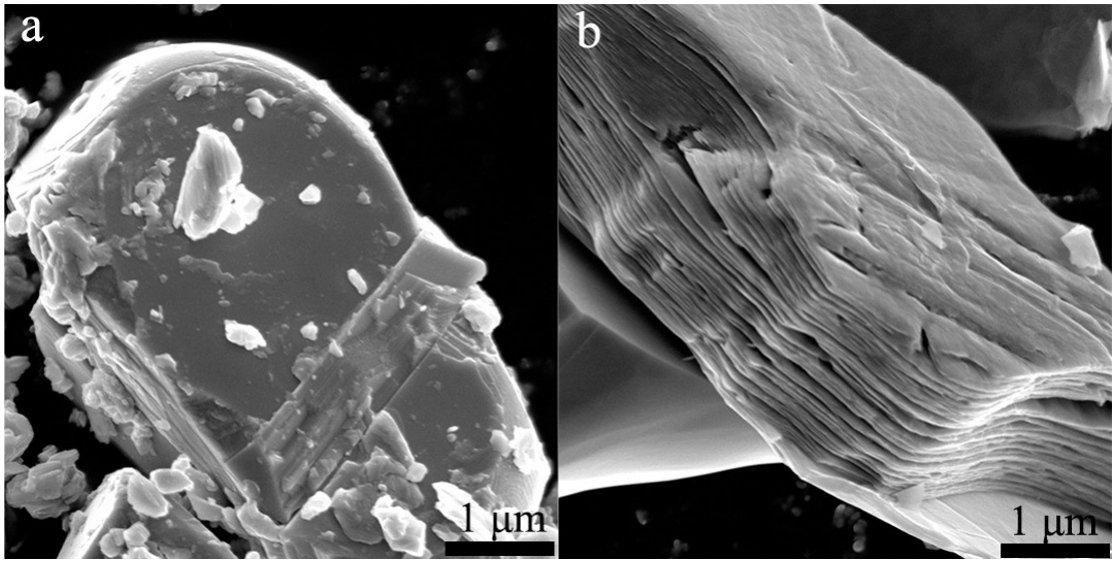

Fig. S1. SEM images of (a) Ti_2AlC, (b) Ti_2CTx.

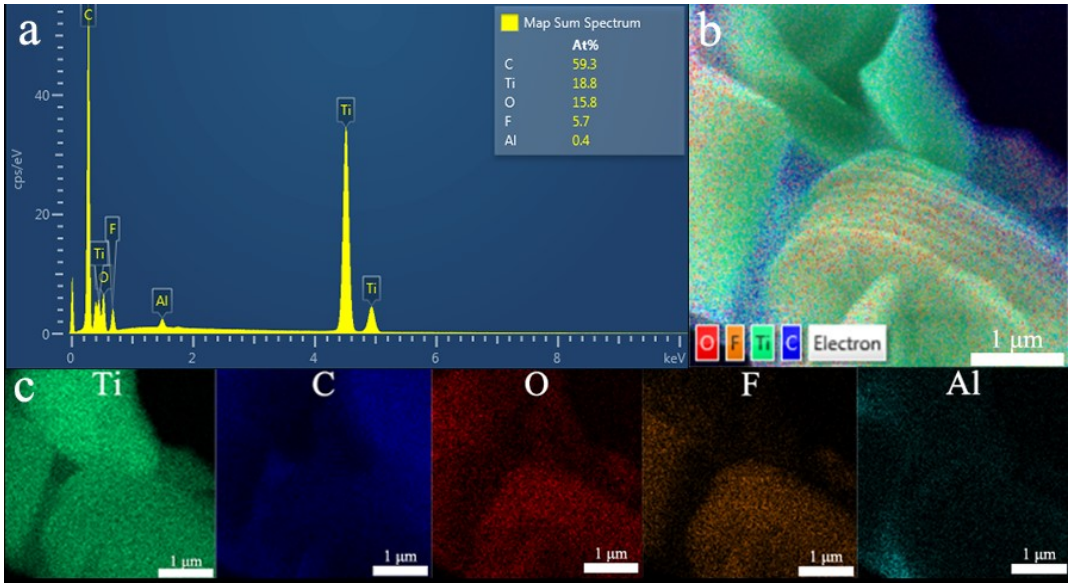

Fig. S2. (a) EDS mapping of Ti_2CT_x. (b-c) EDS elemental mapping of Ti_2CT_x.

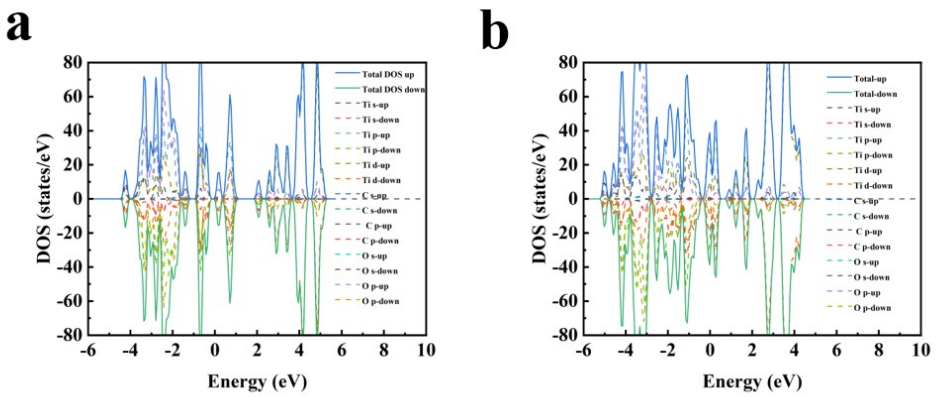

Fig. S3. DOS diagrams for (a) Ti_2CT_x and (b) $Ti_3C_2T_x$.

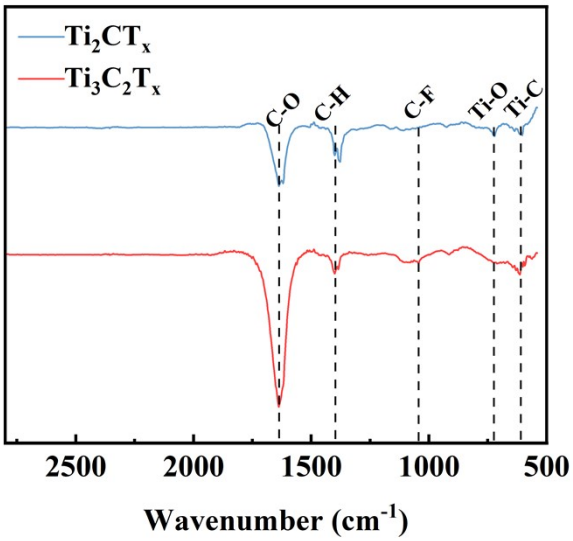

Fig. S4. FTIR spectroscopy of MXenes.

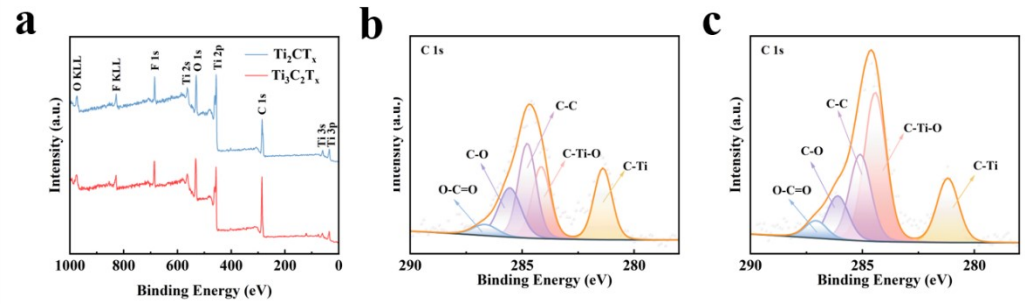

Fig. S5. (a) MXenes full spectra of XPS, C 1s XPS of (b)Ti_2CT_x and (c)$Ti_3C_2T_x$.

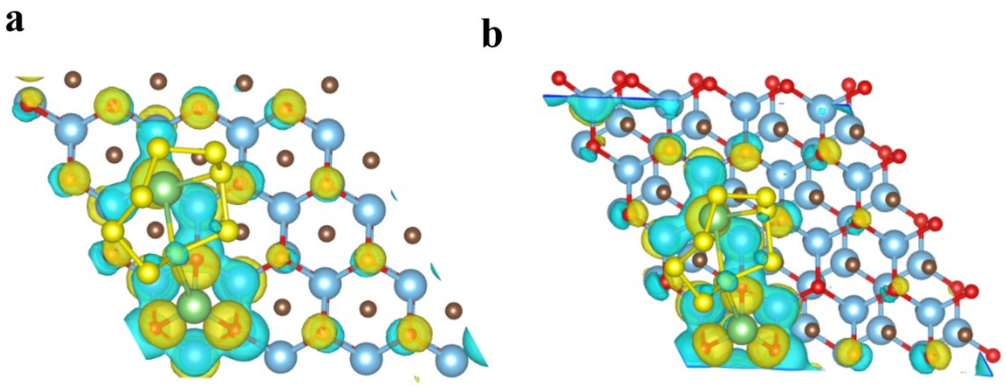

Fig. S6. Top view of the differential charge density for the adsorption of Li_2S_8 on (a) Ti_2CO_2 and (b) $Ti_3C_2O_2$ (Yellow represents electron accumulation; indigo blue represents the electron depletion region)

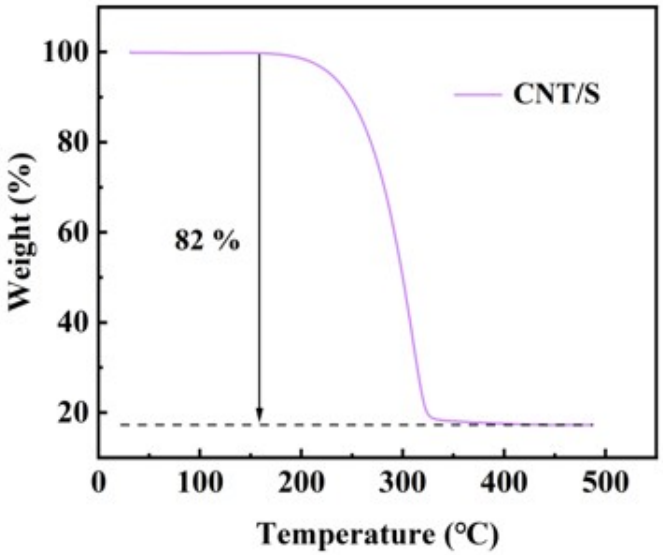

Fig. S7. TGA curves of CNT/S.

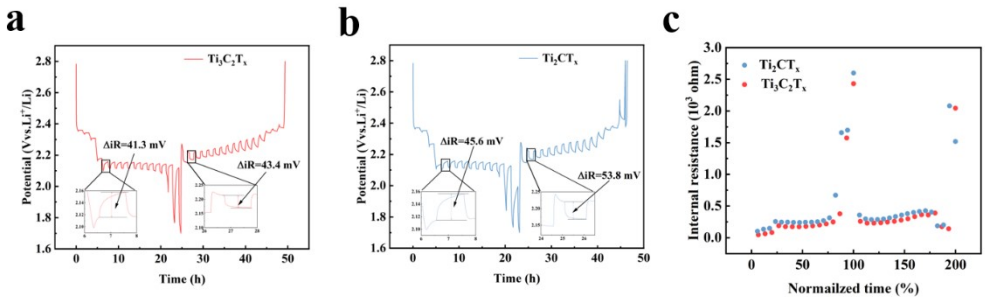

Fig. S8. GITT of (a) $Ti_3C_2T_x$ (b) Ti_2CT_x and corresponding (c) Internal resistance.

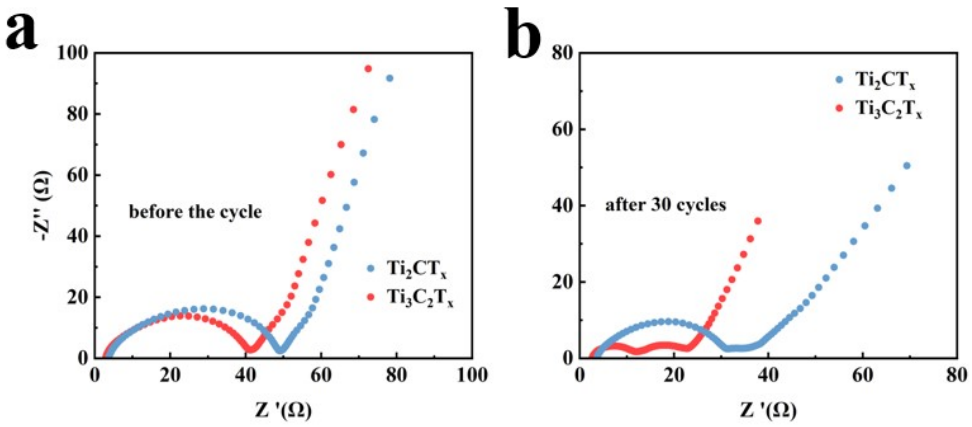

Fig. S9. EIS characterisation of MXenes (a) before the cycle and (b) after 30 cycles.

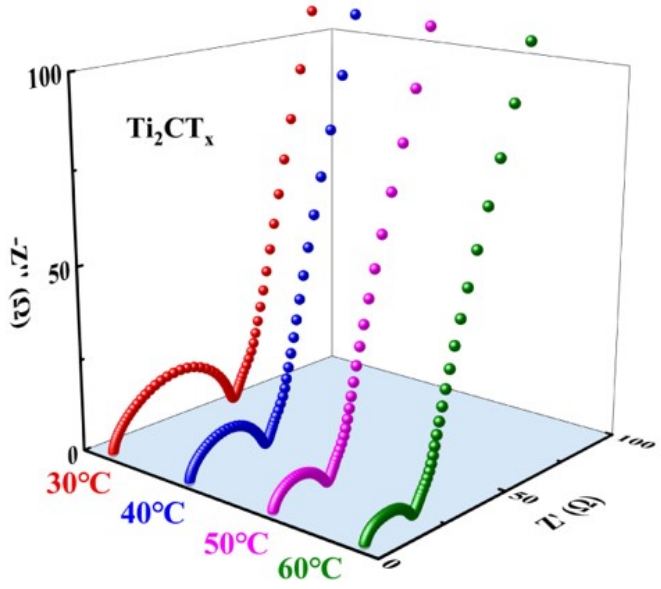

Fig. S10. EIS of Ti_2CT_x at different temperatures.

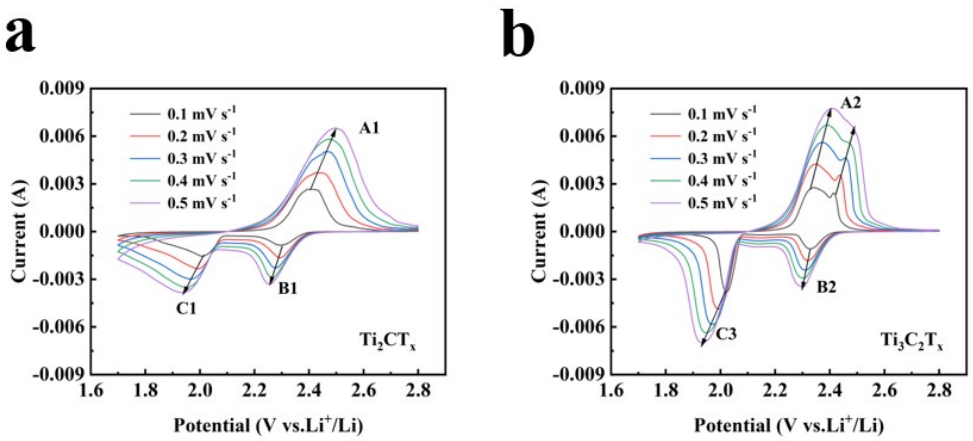

Fig. S11. CV of (a) Ti_2CT_x and (b)$Ti_3C_2T_x$ at different scan rates.

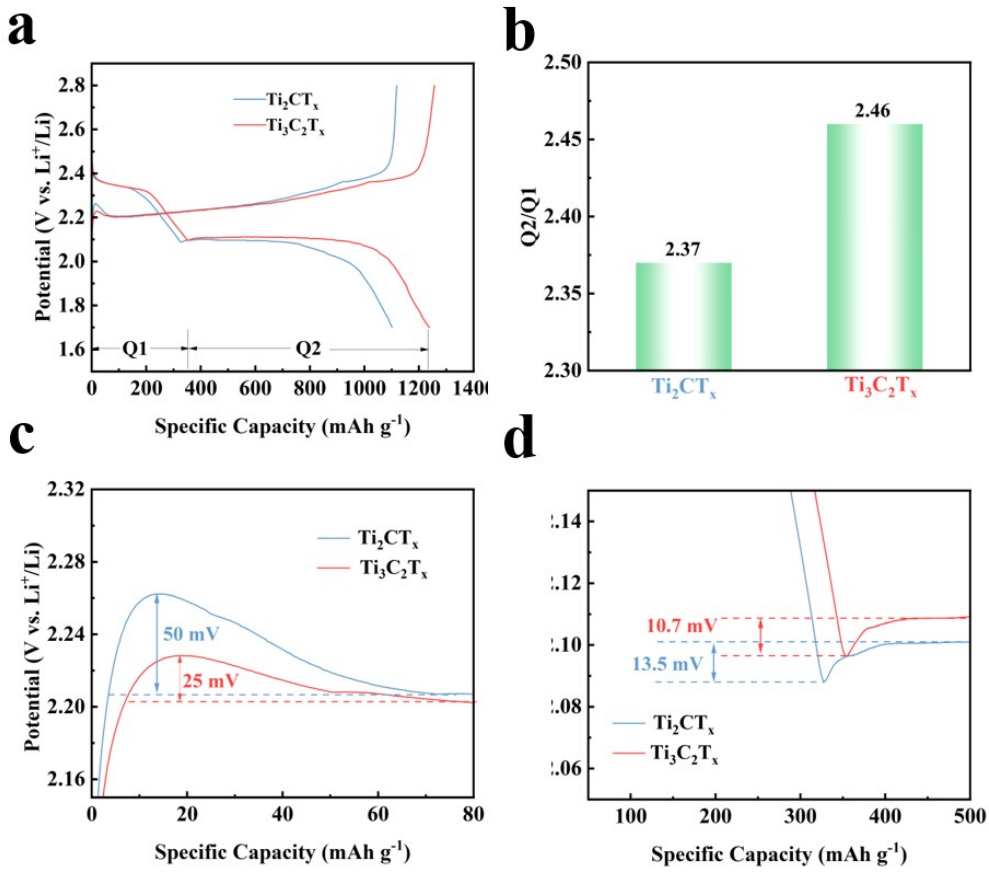

Fig. S12. (a) GCD curves of MXenes. (b)Q2/Q1. (c-d) GCD profiles corresponding enlarged parts.

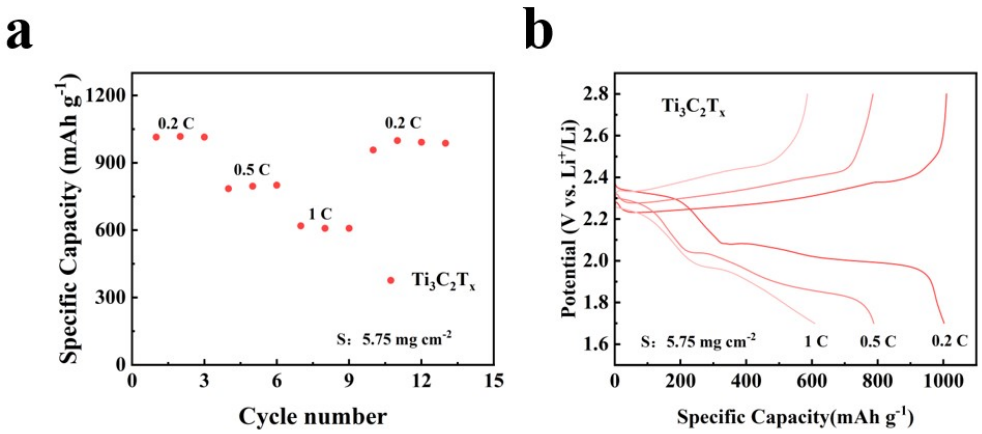

Fig. S13. (a) High-sulfur loading rate performance map of cells with $Ti_3C_2T_x$. (b) corresponding GCD curves

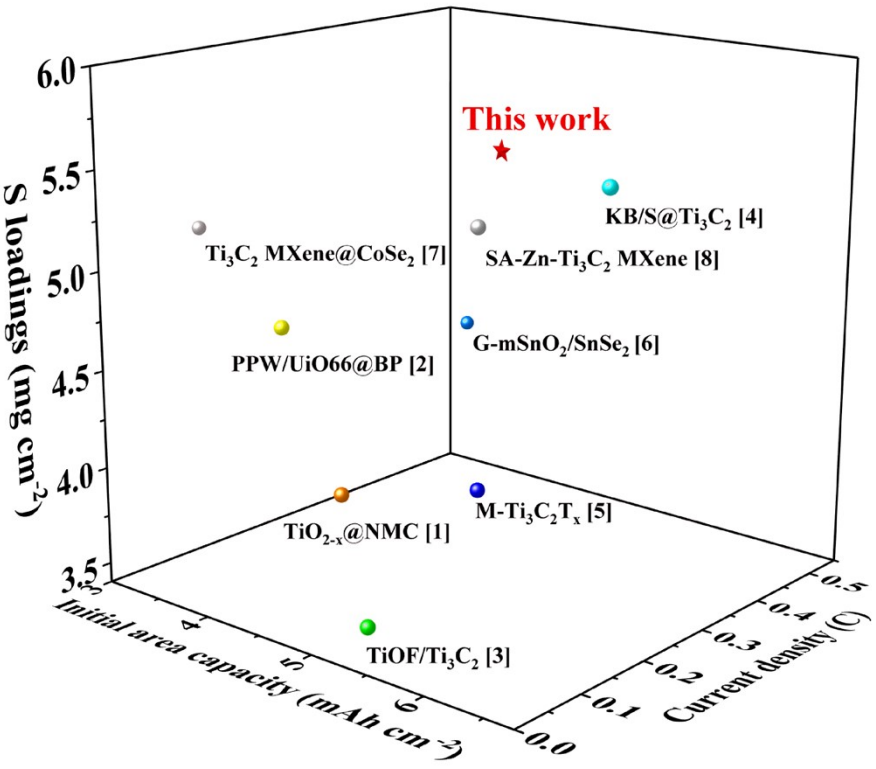

Fig. S14. 3D Performance Comparison Chart

Table S1 O/Ti and F/Ti ratios of MXenes in EDS and XPS.

	EDS:O/Ti	EDS:F/Ti	XPS:O/Ti	XPS:F/Ti
$Ti_3C_2T_x$	0.68	0.37	1.32	0.37
Ti_2CT_x	0.84	0.30	0.87	0.34

Table S2 Cycling and rate performance comparison of $Ti_3C_2T_x$ with commercial carbon-based or TiO_2-coated separators.

Materials	Sulfur loading (mg cm^{-2})	Specific capacity (mAh g^{-1})	Cycle life (cycles)	Ref.
$Ti_3C_2T_x$	1.4	0.1 C-1263 0.2 C-1110 0.5 C-970 1 C-837 2 C-734	200/2 C	This work
TiO_2@p-c-2	0.8	0.2 C-1200 0.5 C-951 1 C-866 2 C-772	100/0.2 C	Ref.9
NCF@TiO_2	1.6	0.05 C-1238 0.1 C-912 0.2 C-805 0.5 C-720 1 C-666	200/0.5 C	Ref.10
NC@CoNiFe/CNTs	2.8	0.1 C-1047 0.2 C-909 0.5 C-856 1 C-793 2 C-697	240/ 0.5 C	Ref.11
CNFs/CoS_{2-x}	1.2~1.3	0.1 C-1167 0.2 C-1074 0.5 C-936 1 C-839 2 C-752	350/1 C	Ref.12
CNT/HEA-NC	1.5	0.1 C-1060 0.2 C-922 0.5 C-819 1 C-744 2 C-676	300/1 C	Ref.13
1T-rich MoS_2@PC	1.3	0.1 C-1076 0.2 C-899 0.5 C-800 1 C-710 2 C-619 3 C-560	500/1 C	Ref.14

Table S3 Comparison of electrochemical performance between $Ti_3C_2T_x$ separators and other MXene/S cathode batteries.

Materials	Application	Sulfur loading (mg cm^{-2})	Specific capacity (mAh g^{-1})/Rate (C)	Ref.
$Ti_3C_2T_x$	Separator	1.4	820 / 1 C	This work
A/R-TiO_2@Ni-N-MXene-S	Cathode	1.5	694 / 1 C	Ref.15
MXene/1T-2H MoS_2-C-S	Cathode	1.0	797 / 1.5 C	Ref.16
OV-TnQDs@PCN/S	Cathode	2.2	718 / 1 C	Ref.17
S@MXene-$CoSe_2$	Cathode	1.0	805 / 1 C	Ref.18
S/Ti_3C_2@N-CNTs	Cathode	1.2	820 / 1 C	Ref.19
TiO_2/H–Ti_3C_2Tx	Cathode	1.0	800 / 1 C	Ref.20

References:

1. J. Zhou, S. Sun, X. Zhou, X. Rao, X. Xu, Z. Zhang, Z. Pan, Q.-C. Wang, Z. Wang, Y. Wu, W. D. Wagner, X. Guo, X. Liu, C. Wang, C. Lu and Y. Zhang, Defect engineering enables an advanced separator modification for high-performance lithium-sulfur batteries, *Chem. Eng. J.*, 2024, **487**, 150574.
2. Y. Huang, Y. Wang and Y. Fu, A thermoregulating separator based on black phosphorus/MOFs heterostructure for thermo-stable lithium-sulfur batteries, *Chem. Eng. J.*, 2023, **454**, 140250.
3. Q. Gu, Y. Cao, J. Chen, Y. Qi, Z. Zhai, M. Lu, N. Huang and B. Zhang, Fluorine-Modulated MXene-Derived Catalysts for Multiphase Sulfur Conversion in Lithium–Sulfur Battery, *Nano-Micro Lett.*, 2024, **16**, 266.
4. Y.-H. Liu, C.-Y. Wang, S.-L. Yang, F.-F. Cao and H. Ye, 3D MXene architectures as sulfur hosts for high-performance lithium-sulfur batteries, *J. Energy Chem.*, 2022, **66**, 429-439.
5. T. Zhang, W. Shao, S. Liu, Z. Song, R. Mao, X. Jin, X. Jian and F. Hu, A flexible design strategy to modify $Ti_3C_2T_x$ MXene surface terminations via nucleophilic substitution for long-life Li-S batteries, *J. Energy Chem.*, 2022, **74**, 349-358.
6. W. Yao, J. Xu, Y. Cao, Y. Meng, Z. Wu, L. Zhan, Y. Wang, Y. Zhang, I. Manke, N. Chen, C. Yang and R. Chen, Dynamic Intercalation–Conversion Site Supported Ultrathin 2D Mesoporous SnO_2/$SnSe_2$ Hybrid as Bifunctional Polysulfide Immobilizer and Lithium Regulator for Lithium–Sulfur Chemistry, *ACS Nano*, 2022, **16**, 10783-10797.
7. T. Li, L. Liang, Z. Chen, J. Zhu and P. Shen, Hollow Ti3C2Tx MXene@$CoSe_2$/N-doped carbon heterostructured composites for multiphase electrocatalysis process in lithium-sulfur batteries, *Chem. Eng. J.*, 2023, **474**, 145970.
8. D. Zhang, S. Wang, R. Hu, J. Gu, Y. Cui, B. Li, W. Chen, C. Liu, J. Shang and S. Yang, Catalytic

Conversion of Polysulfides on Single Atom Zinc Implanted MXene toward High-Rate Lithium–Sulfur Batteries, *Adv. Funct. Mater.*, 2020, **30**, 2002471.

9. X. Luo, Z. Pu, H. Li, E. Zhao, X. Yang, A. Fu, X. Liu, Y.-G. Guo and H. Li, Preparation of TiO_2 nanoparticles decorated porous carbon via a pseudo co-templating strategy and their application as substrates for high performance cathode of Li-S batteries, *J. Energy Storage*, 2024, **102**, 114219.

10. Q. Su, X. Yin, Y. He, Z. Hu, J. Guo, M. Xiang, X. Liu and W. Bai, TiO_2/CNTs dual-decorated functional carbon foam as self-supporting sulfur host for boosting the adsorption and redox kinetics of polysulfides, *J. Alloys Compd.*, 2025, **1010**, 178225.

11. J. Shang, C. Ma, C. Zhang, W. Zhang, B. Shen, F. Wang, S. Guo and S. Yao, Nitrogen-doped carbon encapsulated trimetallic CoNiFe alloy nanoparticles decorated carbon nanotube hybrid composites modified separator for lithium-sulfur batteries, *J. Energy Storage*, 2024, **82**, 110552.

12. X. Men, T. Deng, X. Li, L. Huang and J. Wang, Electrospun carbon nanofibers loaded with sulfur vacancy CoS_2 as separator coating to accelerate sulfur conversion in Lithium-Sulfur batteries, *J. Colloid Interface Sci.*, 2025, **678**, 345-354.

13. Y. Ma, Y. Ren, D. Sun, B. Wang, H. Wu, H. Bian, J. Cao, X. Cao, F. Ding, J. Lu and X. Meng, High entropy alloy nanoparticles dual-decorated with nitrogen-doped carbon and carbon nanotubes as promising electrocatalysts for lithium–sulfur batteries, *J. Mater. Sci. Technol.*, 2024, **188**, 98-104.

14. L.-J. He, J. Liu, T.-T. Lv, A.-C. Wei and T.-Q. Yuan, 1T-rich MoS_2 nanosheets anchored on conductive porous carbon as effective polysulfide promoters for lithium–sulfur batteries, *J. Colloid Interface Sci.*, 2024, **671**, 175-183.

15. Q. Gu, Y. Cao, J. Chen, Y. Qi, Z. Zhai, M. Lu, N. Huang and B. Zhang, Fluorine-Modulated MXene-Derived Catalysts for Multiphase Sulfur Conversion in Lithium–Sulfur Battery, *Nano-Micro Lett.*, 2024, **16**, 266.

16. Y. Zhang, Z. Mu, C. Yang, Z. Xu, S. Zhang, X. Zhang, Y. Li, J. Lai, Z. Sun, Y. Yang, Y. Chao, C. Li, X. Ge, W. Yang and S. Guo, Rational Design of MXene/1T-2H MoS_2-C Nanohybrids for High-Performance Lithium–Sulfur Batteries, *Adv. Funct. Mater.*, 2018, **28**, 1707578.

17. H. Zhang, L. Yang, P. Zhang, C. Lu, D. Sha, B. Yan, W. He, M. Zhou, W. Zhang, L. Pan and Z. Sun, MXene-Derived TiO_2 Quantum Dots Distributed on Porous Carbon Nanosheets for Stable and Long-Life Li–S Batteries: Enhanced Polysulfide Mediation via Defect Engineering, *Adv. Mater.*, 2021, **33**, 2008447.

18. W. Y. Lieu, C. Lin, X. L. Li, S. Jiang, Y. Li, H. Y. Yang and Z. W. Seh, Structural Design of Electrocatalyst-Decorated MXenes on Sulfur Spheres for Lithium–Sulfur Batteries, *Nano Lett.*, 2023, **23**, 5762-5769.

19. R. Liu, S. Zhai, Z. Ye, M. Liu, Y. Xu, C. Li, X. Wang and T. Mei, Constructing carbon nanotube-optimized hollow Ti_3C_2 MXene hierarchical conductive networks for robust lithium–sulfur batteries, *J. Mater. Chem. A*, 2023, **11**, 24330-24337.

20. X. Zhong, D. Wang, J. Sheng, Z. Han, C. Sun, J. Tan, R. Gao, W. Lv, X. Xu, G. Wei, X. Zou and G. Zhou, Freestanding and Sandwich MXene-Based Cathode with Suppressed Lithium Polysulfides Shuttle for Flexible Lithium–Sulfur Batteries, *Nano Lett.*, 2022, **22**, 1207-1216.